American Mineralogist, Volume 90, pages 1861–1870, 2005

High-resolution ^{17}O MAS NMR spectroscopy of forsterite (α-Mg_2SiO_4), wadsleyite (β-Mg_2SiO_4), and ringwoodite (γ-Mg_2SiO_4)

SHARON E. ASHBROOK,[1] ANDREW J. BERRY,[2] WILLIAM O. HIBBERSON,[2] STEFAN STEUERNAGEL,[3] AND STEPHEN WIMPERIS[4,*]

[1]Department of Earth Sciences, University of Cambridge, Downing Street, Cambridge CB2 3EQ, U.K.
[2]Research School of Earth Sciences, Australian National University, Canberra ACT 0200, Australia
[3]Bruker BioSpin GmbH, Am Silberstreifen, 76287 Rheinstetten, Germany
[4]Department of Chemistry, University of Exeter, Stocker Road, Exeter EX4 4QD, U.K.

ABSTRACT

The high sensitivity of the satellite-transition (ST) MAS NMR technique was exploited to obtain high-resolution ^{17}O MAS NMR spectra of the three polymorphs of Mg_2SiO_4: forsterite (α-Mg_2SiO_4), wadsleyite (β-Mg_2SiO_4), and ringwoodite (γ-Mg_2SiO_4). High NMR sensitivity was important in this application because ^{17}O-enriched, Fe-free materials are required for ^{17}O NMR and high-pressure syntheses of the dense β and γ polymorphs result in a only a few milligrams of these solids. In all, eight distinct O species were identified and assigned: three in forsterite, four in wadsleyite, and one in ringwoodite, in agreement with the number of O sites in their crystal structures. The isotropic chemical shifts extracted are in excellent agreement with a previously published correlation with Si-O bond length. However, unexpectedly large quadrupolar coupling constants were found for the non-bridging O species in the dense polymorphs wadsleyite and ringwoodite.

INTRODUCTION

The principal compositional component of the Earth's mantle to a depth of 660 km, $(Mg,Fe)_2SiO_4$, undergoes a series of phase transitions with increasing depth (or pressure). These result in three polymorphs: olivine, α-$(Mg,Fe)_2SiO_4$, is the stable form from the surface to a depth of 410 km; wadsleyite, β-$(Mg,Fe)_2SiO_4$, occurs from 410 to 530 km; while ringwoodite, γ-$(Mg,Fe)_2SiO_4$, is stable between 530 and 660 km (Ringwood 1975; Katsura and Ito 1989). The stability field of the α polymorph is believed to define the extent of the upper mantle, with the transformation of the α to β and β to γ phases resulting in the narrow transition zone between the upper and lower mantle. At greater pressures, in the lower mantle, γ-$(Mg,Fe)_2SiO_4$ disproportionates into (Mg,Fe)O (magnesiowüstite) and a $(Mg,Fe)SiO_3$ perovskite. The physical properties of the upper mantle and transition zone (such as seismic wave velocities, viscosity, compressibility, thermal conductivity, etc.) are thus dominated by the behavior of the three polymorphs of $(Mg,Fe)_2SiO_4$. In this nuclear magnetic resonance (NMR) study, we are concerned solely with the Fe-free forms of olivine, wadsleyite, and ringwoodite; these are termed forsterite (α-Mg_2SiO_4), Mg-rich wadsleyite (β-Mg_2SiO_4), and Mg-rich ringwoodite (γ-Mg_2SiO_4), respectively. For convenience, however, β-Mg_2SiO_4 and γ-Mg_2SiO_4 will hereafter be referred to simply as wadsleyite and ringwoodite.

There are significant differences between the crystal structures of the three Mg_2SiO_4 polymorphs. Forsterite (Hazen 1976) and ringwoodite (Sasaki et al. 1982) contain orthosilicate (SiO_4^{4-}) structural units and each O atom is approximately tetrahedrally coordinated to one Si and three Mg atoms. Forsterite contains three O sites (one O1, one O2, and two O3), while ringwoodite possesses a single O site. Wadsleyite (Horiuchi and Sawamoto 1981), however, contains pyrosilicate ($Si_2O_7^{6-}$) groups resulting in one approximately trigonal-planar bridging O species (O2, coordinated to one Mg and two Si atoms), two distinct tetrahedrally coordinated sites (two O3 and four O4) and an O site (O1) that is not bonded to Si but is coordinated by five Mg atoms in a distorted square-pyramidal geometry. The coordination environments of the O sites in the three polymorphs are shown in Figure 1.

Of particular recent interest is the structural incorporation of water at defect sites in these phases (Kohlstedt et al. 1996; Bolfan-Casanova et al. 2000), which has implications for mantle geodynamics (Hirth and Kohlstedt 1996) owing to the resulting changes in physical properties. The water capacity of the three polymorphs varies considerably. Samples of mantle olivine have been found to contain up to 0.02 wt% water (Bell et al. 2003), although 0.002 wt% is more typical (Bell and Rossman 1992). In contrast, wadsleyite (up to 3.3 wt%) and ringwoodite (up to 2.7 wt%) appear to have much higher affinity for water (Kohlstedt et al. 1996; Smyth 1994). Together, these three polymorphs represent a huge potential reservoir for water given the volume of the upper mantle and transition zone.

The water defect sites and incorporation mechanisms for the three polymorphs are yet to be fully identified. In the highly hydrated forms of wadsleyite and ringwoodite, hydrogen is ordered in the structure and single crystal X-ray diffraction has been used to determine the hydrogen position (Kudoh et al. 1996, 2000;

* E-mail: s.wimperis@ex.ac.uk

0003-004X/05/1112–1861$05.00/DOI: 10.2138/am.2005.1915

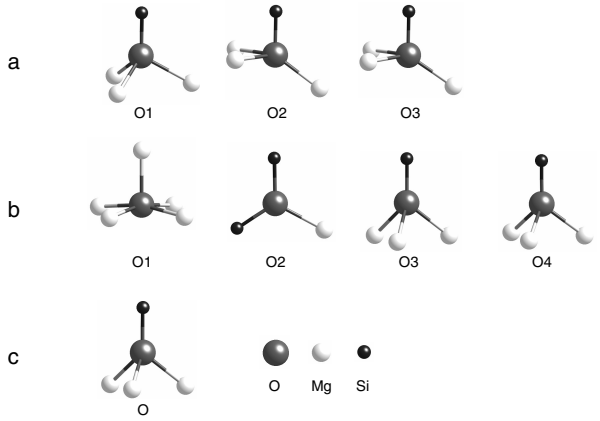

FIGURE 1. O coordination environments in (**a**) forsterite (α-Mg_2SiO_4), (**b**) wadsleyite (β-Mg_2SiO_4), and (**c**) ringwoodite (γ-Mg_2SiO_4).

Smyth et al. 1997). However, at lower water contents, such as in forsterite, the absence of ordering prevents application of diffraction techniques. Furthermore, hydrous wadsleyite (and, potentially, ringwoodite) may be highly disordered and contain a large number of hydrogen sites (Kohn et al. 2002). The ability of NMR to obtain nucleus-specific local structural information, even in the absence of long-range order, offers great potential for the study of these hydrous minerals. Both ^{29}Si and ^{1}H NMR have been used to study the Mg_2SiO_4 polymorphs (Kohn 1996; Kohn et al. 2002; Phillips et al. 1997). ^{29}Si NMR provides information on the local Si environment, but provides little insight into the position of hydrogen in hydrous minerals. The use of ^{1}H NMR, whilst providing direct information on hydrogen, may be hindered by the presence of a significant "background" signal, either from the rotor or water adsorbed onto the mineral surface (Keppler and Rauch 2000). Moreover, information on specific O-H pairings, i.e., the exact location of protons in the lattice, is not directly available.

^{17}O NMR appears to offer a promising alternative for the study of both hydrous and anhydrous minerals and it has the ability (either on its own or in ^{17}O-^{1}H double-resonance experiments) to provide information about direct O-H linkages (Walter et al. 1988; Ashbrook et al. 2001, 2002). However, the ability of ^{17}O NMR to provide detailed information is hampered by both its low natural abundance (~0.037%) and, owing to ^{17}O possessing a spin quantum number, *I*, of 5/2, the presence of a significant quadrupolar broadening (Ganapathy et al. 1982; Vega 1996). The first problem may be overcome for synthetic samples through the use of ^{17}O isotopic enrichment, although owing to the high pressures and high temperatures required for the synthesis of wadsleyite and ringwoodite, only small quantities of these materials (a few milligrams) can usually be prepared. However, the second problem represents a more fundamental difficulty. The technique of magic angle spinning (MAS), widely used to improve resolution in solid-state NMR, is able to remove the quadrupolar interaction to a first-order approximation but is unable to fully remove second-order quadrupolar broadening. Hence, ^{17}O NMR resonances remain broadened, and resolution impaired, even under MAS. Much attention, therefore, has been focused on the complete removal of this broadening through techniques such as dynamic angle spinning (DAS) (Samoson et al. 1988), double rotation (DOR) (Llor and Virlet 1988), and, more recently, multiple-quantum MAS (MQMAS) (Frydman and Harwood 1995).

Forsterite has been studied previously by ^{17}O MAS NMR (Schramm and Oldfield 1984) and truly high-resolution spectra have been obtained using DAS and DOR (Mueller et al. 1991, 1992). More recently, a complete assignment of the high-resolution ^{17}O NMR spectrum of forsterite was achieved with the aid of MQMAS (Ashbrook et al. 1999). This technique is perhaps the most commonly used method for obtaining high-resolution MAS NMR spectra of quadrupolar nuclei as it may be implemented (unlike DAS and DOR) with conventional MAS probeheads. However, the MQMAS technique has severely limited sensitivity, particularly at high MAS rates and in the presence of large quadrupolar interactions. Although useful in the case of forsterite, the small amounts of the high-pressure Mg_2SiO_4 polymorphs available precluded the use of this technique and a more sensitive method was required. The satellite-transition MAS (STMAS) experiment (Gan 2000) was introduced as an alternative, and more sensitive, method for obtaining high-resolution quadrupolar NMR spectra. Although STMAS is technically more difficult to implement than MQMAS, owing to the stringent requirements for both a stable spinning rate and a spinning axis set accurately (±0.002°) to the magic angle (54.736°) (Gan 2000; Pike et al. 2001; Ashbrook and Wimperis 2002, 2004), it can be successfully implemented on most conventional MAS probes. Recently, we have obtained the first high-resolution ^{17}O MAS NMR spectrum of wadsleyite (~10 mg, isotopically enriched to 35% in ^{17}O), demonstrating the excellent sensitivity of the STMAS technique (Ashbrook et al. 2003).

The compositional similarity but structural variability of the three Mg_2SiO_4 polymorphs is ideal for investigating the relationship between the NMR parameters (γ_{CS}, the isotropic chemical shift, and C_Q and η, the magnitude and asymmetry of the quadrupolar interaction tensor, respectively) and structure. In this work, we characterize and compare ^{17}O NMR spectra of the three anhydrous polymorphs (isotopically enriched to 35% in ^{17}O), which is an essential prerequisite to the study of the hydrous materials. The use of STMAS for the acquisition and interpretation of high-resolution ^{17}O NMR spectra will be demonstrated using forsterite as a model sample before the two denser polymorphs are discussed.

EXPERIMENTAL DETAILS

The Mg_2SiO_4 polymorphs were synthesized from ^{17}O-enriched (35%) MgO and SiO_2 prepared from the reaction of $H_2{}^{17}O$ with Mg_3N_2 and $SiCl_4$, respectively (Ashbrook et al. 1999). Forsterite was produced at 1500 °C and atmospheric pressure (Ashbrook et al. 1999), and then converted into wadsleyite at 16 GPa and 1600 °C (Ashbrook et al. 2003) and ringwoodite at 20 GPa and 1200 °C (2 hours) using a MA8-type multi-anvil apparatus (Grey et al. 1999). At these pressures only mg quantities of material could be prepared in a single experiment: ~10 mg of wadsleyite in two sealed Pt capsules and ~5 mg of (nominal) ringwoodite in a single capsule. The phase purity of each sample was assessed by X-ray diffraction, with the resulting data shown in Figure. 2.

^{17}O MAS NMR spectra were obtained at Larmor frequencies of 54.2 MHz, 67.8 MHz, 81.4 MHz, and 108.5 MHz on Bruker Avance spectrometers equipped with 9.4 T, 11.7 T, 14.1 T, and 18.8 T magnets, respectively. Powdered samples were packed into 2.5 mm rotors and MAS rates of between 20 and 30 kHz were used. For wadsleyite and ringwoodite, the total amount of solid filled less than a quarter of the rotor and so an inert spacer was employed to ensure that it lay in the

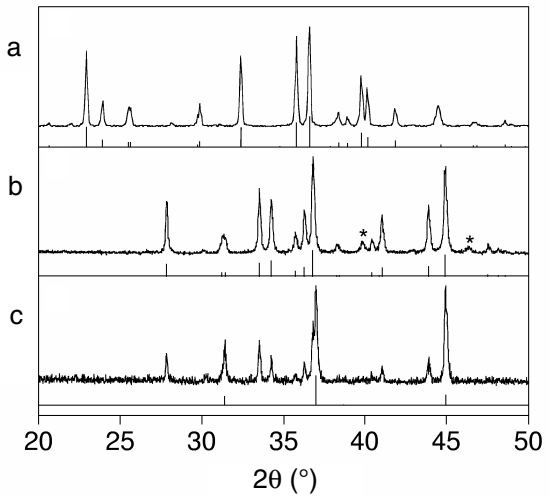

FIGURE 2. Cu$K\alpha$ X-ray diffraction powder patterns for (**a**) forsterite, (**b**) wadsleyite, and (**c**) ringwoodite (with a significant wadsleyite impurity). The * in (**b**) indicates Pt from the capsule.

center of the radiofrequency coil. Two -dimensional STMAS NMR experiments were performed using a phase-modulated split-t_1 shifted-echo pulse sequence (Pike et al. 2001; Ashbrook and Wimperis 2002, 2004). The spinning angle was adjusted prior to the experiment to 54.736° ± 0.002° using ^{87}Rb NMR of a rotor filled with $RbNO_3$ (Ashbrook and Wimperis 2002, 2004). This material was also used as the inert spacer in the rotor enabling the spinning angle to be accurately monitored throughout. ^{29}Si MAS NMR spectra were acquired at a Larmor frequency of 79.5 MHz with a Bruker Avance spectrometer equipped with a 9.4 T magnet. The ^{17}O and ^{29}Si ppm scales are referenced to H_2O (^{17}O) and TMS (^{29}Si), respectively. Further experimental details can be found in the figure captions.

RESULTS

Forsterite (α-Mg_2SiO_4)

The ^{29}Si (79.5 MHz) and ^{17}O (54.2 MHz) MAS NMR spectra of ~50 mg of forsterite are shown in Figures 3a and 4a, respectively. A single sharp resonance is observed in the ^{29}Si spectrum with an isotropic chemical shift of approximately –61 ppm, in agreement with that reported previously (Magi et al. 1984). This chemical shift is typical of a Q^0 Si species (in Q^n notation, n is the number of bridging oxygen atoms, i.e., Si-O-Si, coordinated to Si), as found in the isolated SiO_4^{4-} units of the forsterite structure (Engelhardt 1996). In contrast, the ^{17}O (54.2 MHz) MAS NMR spectrum of forsterite is considerably more complicated, displaying a broad line shape centered on ~50 ppm. The broadening observed, resulting from the interaction of the ^{17}O nuclear quadrupole moment and the electric field gradient (EFG) across the nucleus, is second-order in nature and hence is not removed by MAS alone. This complicates the interpretation of the NMR spectrum and hinders the extraction of any information on the number and nature of crystallographically distinct oxygen species (Ganapathy et al. 1982; Vega 1996).

A two-dimensional ^{17}O (54.2 MHz) STMAS NMR spectrum of forsterite is shown in Figure 4b. As the second-order quadrupolar broadening is refocused at the end of the t_1 period using this technique, the spectrum consists of a series of ridge line shapes lying parallel to the δ_2 axis. A projection orthogonal to these line shapes, i.e., onto the δ_1 axis, yields a high-resolution or "isotro-

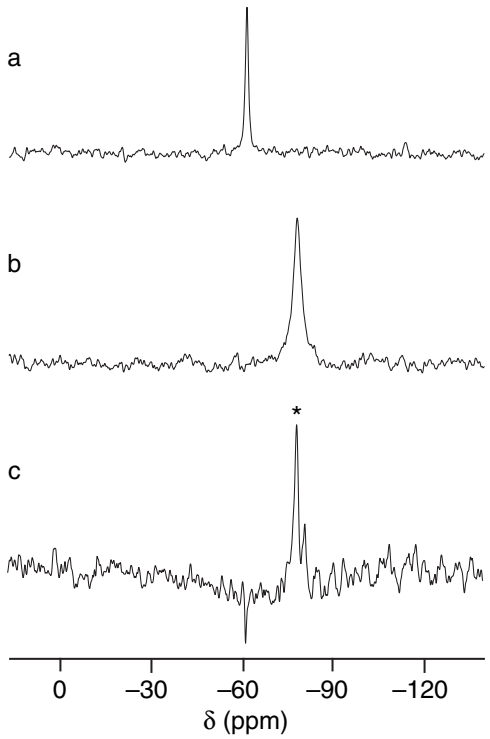

FIGURE 3. ^{29}Si MAS NMR spectra of (**a**) forsterite, (**b**) wadsleyite, and (**c**) ringwoodite (with a significant wadsleyite impurity, indicated by *). Spectra recorded at a magnetic field strength, B_0, of 9.4 T and a MAS rate of 20 kHz. The number of transients averaged was (**a**) 80, (**b**) 2700, and (**c**) 17 000. The relaxation interval was 20 s.

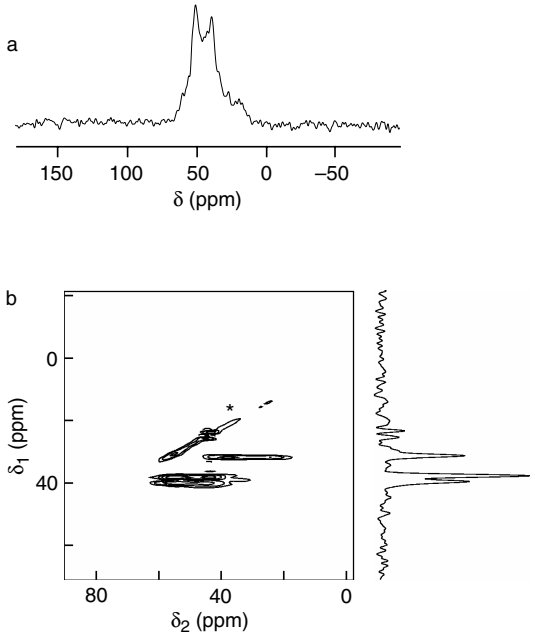

FIGURE 4. ^{17}O NMR spectra of forsterite recorded at B_0 = 9.4 T and a MAS rate of 20 kHz. (**a**) Conventional MAS spectrum: 100 transients averaged with a relaxation interval of 2 s. (**b**) Two-dimensional STMAS spectrum and corresponding isotropic projection: 128 transients averaged with a relaxation interval of 1 s for each of 256 t_1 increments of 64.58 µs. Contour levels are drawn at 8, 16, 32, and 64% of the maximum value. The * in (**b**) marks the central-transition autocorrelation ridge.

pic" spectrum. This displays three sharp, narrow resonances, corresponding to the three crystallographically distinct O species present in the structure, with intensities in the ratio of 1:2:1 in order of increasing δ_1 shift. It should be noted that the efficiency of the STMAS experiment varies as a function of the quadrupolar interaction, with a decrease in sensitivity encountered as C_Q (the quadrupolar coupling constant or magnitude of the quadrupolar interaction) increases. However, the relatively small differences in quadrupolar interaction between the three distinct oxygen species in forsterite enables the site populations to be determined directly from the relative intensities of the resonances in the isotropic spectrum (Ashbrook et al. 1999). In addition to the three ridges described, the two-dimensional spectrum also contains a further diagonal ridge signal (marked with an asterisk in Fig. 4b), resulting from correlation, not between satellite and central transitions, but between the central transition in both the δ_1 and δ_2 dimensions, i.e., it is an uninformative autocorrelation signal (Gan 2000; Ashbrook and Wimperis 2004).

In addition to the acquisition of a high-resolution NMR spectrum, the two-dimensional nature of the STMAS experiment ensures that the quadrupolar and chemical shift information is also retained. This can be determined by two methods. In the first, the isotropic chemical shift, δ_{CS}, and a second-order quadrupolar shift, δ_Q, are extracted by analysis of the position of the center-of-mass (COM) of each line shape in the δ_1 and δ_2 dimensions. For a spin $I = 5/2$ STMAS spectrum, recorded using a split-t_1 technique and using a rational convention for axis labeling (Ashbrook and Wimperis 2004), the δ_1 and δ_2 shifts of the center-of-mass of a two-dimensional line shape are given by

$$\delta_1^{COM} = (17/31)\,\delta_{CS} + (32/93)\,\delta_Q \quad (1)$$
$$\delta_2^{COM} = \delta_{CS} - (16/15)\,\delta_Q. \quad (2)$$

By rearranging we obtain,

$$\delta_{CS} = (31\delta_1^{COM} + 10\delta_2^{COM})/27 \quad (3)$$
$$\delta_Q = 5\,(31\delta_1^{COM} - 17\delta_2^{COM})/144. \quad (4)$$

Thus, if δ_1^{COM} and δ_2^{COM} are measured then both δ_{CS} and δ_Q may be determined. It should be noted that from δ_Q alone the quadrupolar parameters, C_Q and η, cannot be determined separately. However, the quadrupolar product, P_Q, given by (Mueller et al. 1992)

$$P_Q = C_Q\,[1 + (\eta^2/3)]^{1/2}, \quad (5)$$

can be obtained from δ_Q by

$$P_Q = \frac{4I(2I-1)\nu_0\sqrt{\delta_Q}}{3000} \quad (6)$$

where ν_0 is the Larmor frequency in Hz (Ashbrook and Wimperis 2004). The values of δ_{CS} and P_Q extracted in this manner for the three oxygen species in forsterite are given in Table 1.

In the second method, the individual quadrupolar parameters C_Q and η (which are perhaps more informative than the quadrupolar product, P_Q) can be determined directly by fitting the second-order quadrupolar-broadened line shapes extracted from cross-sections, parallel to δ_2, through the two-dimensional ridges in the STMAS spectrum. Figure 5a-c shows the line shapes from the three resolved resonances in the ^{17}O STMAS spectrum of forsterite in Figure 4b. The values of C_Q and η obtained from the fitting are given in Table 1, with the computer-generated line shapes shown in Figures 5d–5f. As a check for consistency, the values of P_Q, calculated from C_Q and η, are 2.8, 2.5, and 2.6 MHz, in good agreement with the values derived from the positions of the center-of-mass of the two-dimensional line shapes (Table 1). We note that excellent agreement is obtained between the experimental and simulated line shapes. The small distortions present in the experimental line shapes are probably a consequence of the non-uniform excitation and conversion of the satellite-transition coherences.

The values of the chemical shift and quadrupolar parameters shown in Table 1 enable a full assignment of the resonances in the isotropic ^{17}O MAS NMR spectrum, in agreement with that found previously (Ashbrook et al. 1999). In order of increasing δ_1 shift, they can be identified as O1, O3, and O2. The assignment of O3 is particularly straightforward on the basis of the intensity ratios of the resonances, as the site population of O3 is twice that of O1 and O2. A comparison of the O coordination environment (e.g., Fig. 1a) indicates that the distorted tetrahedral bond angles for O3 and O2 are very similar (Hazen 1976), but quite different to O1, allowing the peak of similar δ_{CS} to be identified as O2,

TABLE 1. ^{17}O isotropic STMAS shifts (δ_1) at B_0 = 9.4 T, isotropic chemical shifts (δ_{CS}), quadrupolar products (P_Q), quadrupolar coupling constants (C_Q), asymmetries (η), relative populations, and assignments of the oxygen species in forsterite, wadsleyite, and ringwoodite

Material	δ_1 (9.4 T) (ppm)	δ_{CS} (ppm)	P_Q/ MHz	C_Q/ MHz	η	Population	Assignment
Forsterite	32(1)	48(1)	2.8(1)	2.8(1)	0.3(1)	1	O1
	37(1)	61(1)	2.4(1)	2.5(1)	0.2(1)	2	O3
	39(1)	64(1)	2.6(1)	2.5(1)	0.4(1)	1	O2
Wadsleyite	22(1)	38(1)	1.3(1)	–	–	1	O1*
	45(1)	65(1)	3.8(1)	3.8(1)	0.3(1)	4	O4
	49(1)	66(1)	4.4(1)	4.4(1)	0.2(1)	2	O3
	62(1)	76(1)	5.6(1)	4.8(1)	0.9(1)	1	O2
Ringwoodite	51(1)	63(1)	4.9(1)	4.8(1)	0.05(5)	1	O

* C_Q and η not determined.

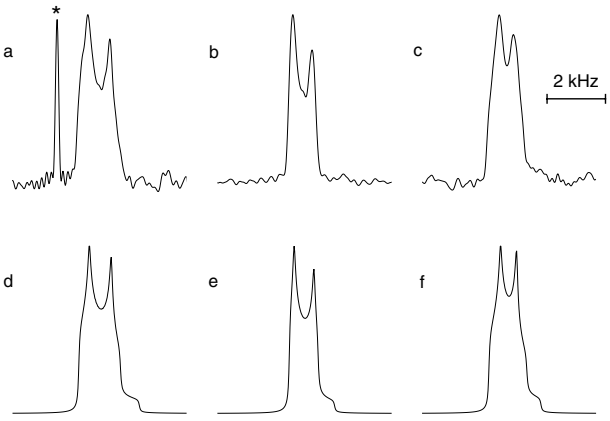

FIGURE 5. (**a**–**c**) Cross-sections parallel to the δ_2 axis through the three second-order broadened ridge line shapes in the forsterite STMAS spectrum in Figure 4b at (**a**) δ_1 = 32 ppm, (**b**) δ_1 = 37 ppm, and (**c**) δ_1 = 39 ppm. (**d**-**f**) Corresponding computer fits, yielding the C_Q and η values given in Table 1. The * in (**a**) indicates where the cross-section passes through the uninformative central-transition autocorrelation peak.

leaving O1 as the resonance with a significantly different value of δ_{CS}. This empirical assignment agrees with a previous theoretical calculation of C_Q and η (Winkler et al. 1996).

The two-dimensional STMAS spectrum of forsterite in Figure 4b was recorded over 9 h and exhibits an excellent signal-to-noise ratio. This result shows, therefore, that the STMAS experiment offers great potential for the acquisition of high-resolution ^{17}O NMR spectra of the more challenging Mg_2SiO_4 polymorphs using a moderate static magnetic field strength, B_0, and within a reasonable time.

Wadsleyite (β-Mg_2SiO_4)

The ^{29}Si (79.5 MHz) MAS NMR spectrum of ~10 mg of wadsleyite, shown in Figure 3b, displays a single resonance at approximately –79 ppm, in agreement with that reported previously (Stebbins and Kanzaki 1991). This chemical shift, significantly more negative than that observed for forsterite, is typical of a Q^1 Si species (Engelhardt 1996), reflecting the presence of $Si_2O_7^{6-}$ units within the structure. As found for forsterite, the ^{17}O MAS NMR spectrum of wadsleyite is considerably more complicated, resulting from the overlap of line shapes from more than one crystallographically distinct species (Ashbrook et al. 2003). The spectrum has a complicated dependence upon the static magnetic field strength, as shown in Figure 6a-d, as the second-order quadrupolar interaction ($\propto B_0^{-1}$) and the chemical shift ($\propto B_0$) have different dependencies upon B_0. It is not possible to resolve all resonances at the magnetic field strengths used here, although at B_0 = 18.8 T (Fig. 6d) one peak does appear to be fully resolved (the narrow resonance at ~37 ppm).

To resolve all the O resonances, a two-dimensional NMR experiment is required. Owing to the small amount of material available (~10 mg), the sensitivity advantage of STMAS over the commonly used MQMAS experiment and its reduced dependence upon the MAS rate makes it the method of choice for the study of wadsleyite. Two-dimensional ^{17}O STMAS NMR spectra recorded at B_0 field strengths of 9.4 T and 11.7 T are shown in Figures 7a and b, respectively (Ashbrook et al. 2003). These spectra were recorded with total experimental times of 70 h (Fig. 7a) and 24 h (Fig. 7b). In each spectrum four distinct ridges are observed lying parallel to the δ_2 axis, corresponding to four distinct oxygen species, in addition to a signal resulting from purely central-transition autocorrelation (marked with an asterisk). One ^{17}O resonance is very sharp and lies close to the autocorrelation signal, reflecting the small quadrupolar interaction of this species. The other three resonances are much broader, with the fourth ridge (at $\delta_1 \approx 62$ ppm in Fig. 7a) not easily observable with the contour levels shown. The isotropic spectra, however, obtained from projections onto the δ_1 dimension, clearly reveal the presence of four distinct resonances (Ashbrook et al. 2003).

It is possible to extract information on the quadrupolar and chemical shift interactions for each individual oxygen species from the spectra using a variety of different methods. As described for forsterite, the position of the center-of-mass of a resonance in an STMAS spectrum is dependent upon both the isotropic chemical shift and a second-order quadrupolar shift. However, although the position of the ridge in the δ_1 dimension (given by δ_1^{COM}) is often easily obtained using the isotropic projection, the determination of the position in the δ_2 dimension, where significant anisotropic broadening is still present, can be difficult if there is not a well-defined second-order line shape. This is often the case when sensitivity is low or when significant distortions are observed as a result of non-quantitative coherence transfer. Fortunately, both the isotropic chemical shift and the second-order quadrupolar shift can also be extracted from a comparison of the δ_1^{COM} values of each resonance as a function of the B_0 field strength. For example, if the δ_1^{COM} (in ppm) of a specific

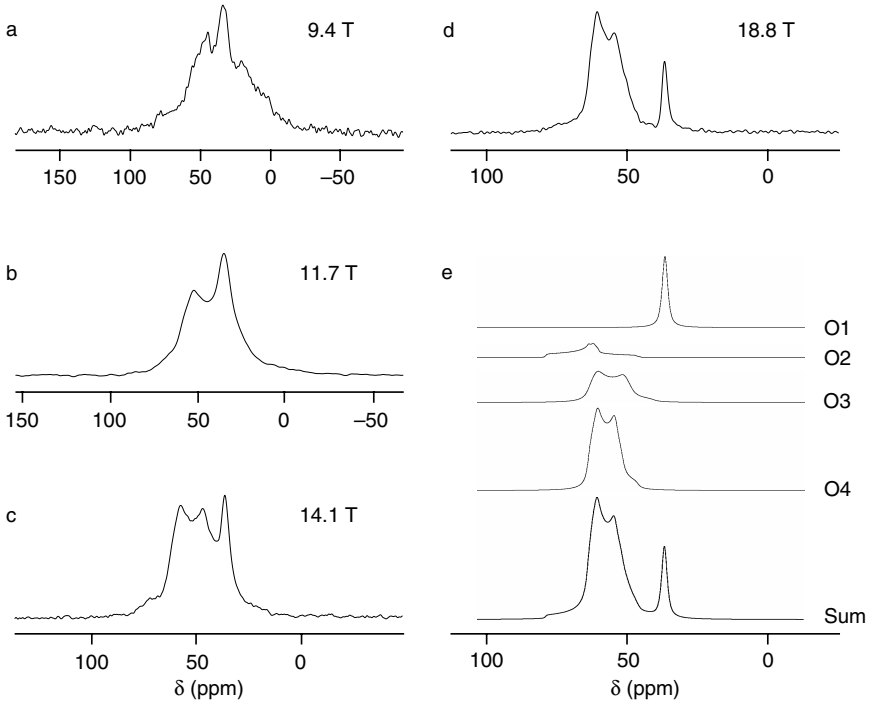

FIGURE 6. (**a**–**d**) Experimental and (**e**) simulated ^{17}O MAS NMR spectra of wadsleyite. Experimental spectra recorded at magnetic field strengths, B_0, of (**a**) 9.4 T, (**b**) 11.7 T, (**c**) 14.1 T, and (**d**) 18.8 T. Number of transients averaged: (**a**) 2000, (**b**) 20480, (**c**) 1600, and (**d**) 2048 with a relaxation interval of (**a**) 2 s and (**b**-**d**) 1 s. The MAS rate was (**a**) 20 kHz and (**b**-**d**) 25 kHz. The computer-generated line shapes in (**e**) were simulated for B_0 = 18.8 T using the quadrupolar and chemical shift parameters for the four O species in Table 1; the sum of the four individual line shapes can be compared with (**d**).

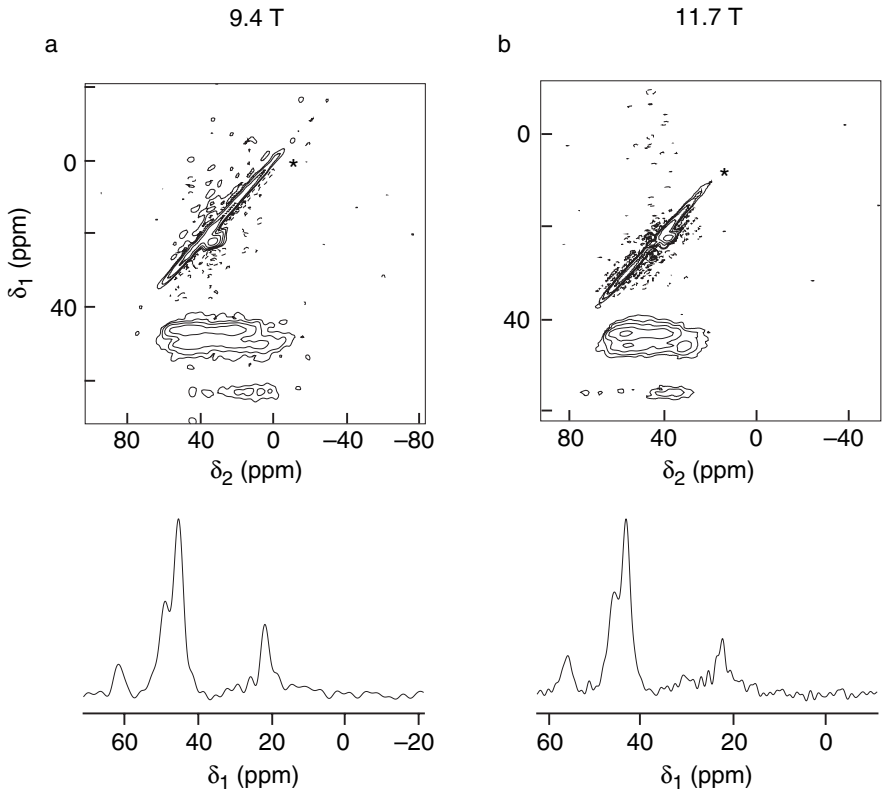

FIGURE 7. Two-dimensional ^{17}O STMAS NMR spectra of wadsleyite and the corresponding isotropic projections, recorded at (**a**) B_0 = 9.4 T and (**b**) B_0 = 11.7 T. Number of transients averaged: (**a**) 1408 and (**b**) 416 with a relaxation interval of (**a**) 2 s and (**b**) 1 s for each of (**a**) 90 and (**b**) 200 t_1 increments of (**a**) 64.6 µs and (**b**) 51.67 µs. The MAS rate was (**a**) 20 kHz and (**b**) 25 kHz. Total experiment times were (**a**) 70 hours and (**b**) 24 hours. Contour levels are drawn at 4, 8, 16, 32, and 64% of the maximum value. The diagonal central-transition autocorrelation ridges are marked with *.

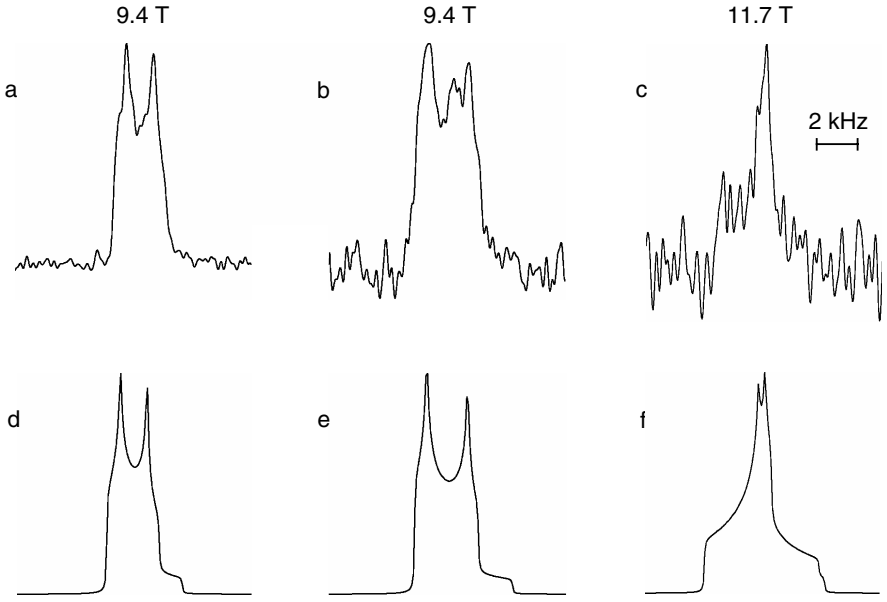

FIGURE 8. (**a**-**c**) Cross-sections parallel to the δ_2 axis through second-order broadened ridge line shapes in wadsleyite STMAS spectra: (**a**) Figure 7a (B_0 = 9.4 T) at δ_1 = 45 ppm, (**b**) Figure 7a (B_0 = 9.4 T) at δ_1 = 49 ppm, and (**c**) Figure 7b (B_0 = 11.7 T) at δ_1 = 58 ppm. (**d**-**f**) Corresponding computer fits, yielding the C_Q and η values given in Table 1.

resonance is plotted against $(1/\nu_0^2)$, where ν_0 is the Larmor frequency in Hz, the result will be (for spin I = 5/2) a straight line with gradient of (60 000/31) P_Q^2 and an intercept of (17/31) δ_{CS}.

The experimental δ_2 cross-sections were fitted to extract C_Q and η. As such an analysis requires a well-defined second-order line shape, this method was not applied to the narrowest ridge as no second-order broadening was apparent in either spectrum. Examples of line shapes extracted from the spectra in Figure 7, along with the corresponding computer fits, are shown in Figure 8.

The values of δ_{CS}, P_Q, C_Q, and η for the four distinct O species in wadsleyite, extracted using a combination of the methods described above, are given in Table 1. As a check for consistency, the ^{17}O MAS spectrum, recorded at B_0 = 18.8 T, was compared with a computer-generated MAS line shape simulated using the values for the four distinct O species given in Table 1 (Ashbrook et al. 2003). The excellent agreement of the sum of these line shapes, shown in Figure 6e, with the ^{17}O MAS spectrum in Figure 6d reflects the accuracy of the values extracted from the STMAS spectra.

An assignment of the ^{17}O STMAS NMR spectrum of wadsleyite is relatively straightforward from a comparison of the crystallographic site populations, which are in the ratio 1:1:2:4 for O1, O2, O3, and O4 respectively, with the relative resonance intensities of approximately, in order of increasing δ_1 shift, 1:4:2:1 (Horiuchi and Sawamoto 1981; Ashbrook et al. 2003). O4 and O3 (non-bridging oxygen atoms with very similar C_Q and δ_{CS} values), were therefore assigned from their relative intensities. The remaining species, O1 and O2, may be distinguished on the basis of their quadrupolar interactions. The O2 oxygen atom, bridging between two Si species in the $Si_2O_7^{6-}$ unit, is expected to exhibit a large quadrupolar interaction (e.g., Ashbrook et

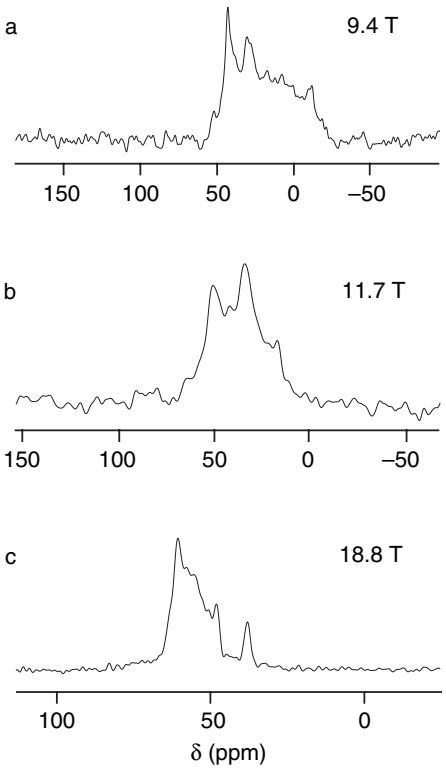

FIGURE 9. ^{17}O MAS NMR spectra of ringwoodite (plus a significant wadsleyite impurity), recorded at magnetic field strengths, B_0, of (**a**) 9.4 T, (**b**) 11.7 T, and (**c**) 18.8 T. In (**a**) 40 000, (**b**) 14 400, and (**c**) 230 400 transients were averaged with a relaxation interval of (**a**) 4 s, (**b**) 1 s, and (**c**) 1 s. The MAS rate was (**a**, **b**) 20 kHz and (**c**) 25 kHz.

al. 2002). The resonance with P_Q = 5.6 MHz, therefore, may be attributed to O2, leaving the remaining resonance, with P_Q = 1.3 MHz, as O1, a five-coordinate O species coordinated only by Mg. This assignment appears consistent with the largely ionic character (and, therefore, relatively symmetrical electronic environment) of this species. The O1 site is of particular interest as it offers a favorable location for hydration, perhaps explaining to some extent the increased affinity of wadsleyite for water when compared with forsterite.

Ringwoodite (γ-Mg_2SiO_4)

The X-ray diffraction data shown in Figure 2c indicate that the ringwoodite sample contains a very significant amount of wadsleyite, arising from incomplete conversion of β- to γ-Mg_2SiO_4. The ^{29}Si MAS NMR spectrum of this ringwoodite sample, recorded with a relaxation interval of 20 s, is shown in Figure 3c and exhibits a strong resonance at –79 ppm and a smaller peak at –82 ppm. The former (marked with an asterisk) corresponds to the wadsleyite impurity. The peak at –82 ppm corresponds to the Si site in ringwoodite, as confirmed by ^{29}Si MAS NMR of a pure, but not ^{17}O-enriched, ringwoodite sample (spectrum not shown). For the amounts of ringwoodite and wadsleyite in the sample, the ringwoodite peak has relatively low intensity in the spectrum in Figure 3c as a result of Si at this site having a much longer spin-lattice relaxation time than the Si in wadsleyite, as confirmed by an experiment with a 60 s relaxation interval (spectrum not shown). It is interesting to note that, although just within the range typical of a Q^0 species, the Si resonance of ringwoodite occurs at a slightly more negative chemical shift than that of the Q^1 species of wadsleyite. The ^{17}O MAS NMR spectra of the ringwoodite sample, recorded at static magnetic field strengths of 9.4, 11.7, and 18.8 T, are shown in Figure 9. Despite the presence of only a single distinct O species in ringwoodite, the spectra display complex line shapes as a result of the presence of the wadsleyite impurity.

To resolve the ringwoodite O species from those of the wadsleyite impurity, two-dimensional ^{17}O STMAS NMR spectra were recorded with B_0 field strengths of 9.4 T and 11.7 T for 132 and 55 h, respectively. These spectra, along with corresponding isotropic projections, are shown in Figure 10. At first sight the two-dimensional spectra seem very similar to those of wadsleyite in Figure 7, with a narrow resonance and two much broader ridge line shapes at higher δ_1 shifts, as expected for the significant wadsleyite impurity present in this sample. It may be presumed that the fourth O species in wadsleyite, at higher δ_1 still, is unobservable at the signal-to-noise levels available. Significant differences between these spectra and those of wadsleyite in Figure 7 are observed, however, in the isotropic projections, which are compared for the spectra recorded with B_0 = 9.4 T in Figure 10a. The resonance at $\delta_1 \approx 45$ ppm (that is assigned to the O4 species in wadsleyite) is clearly present in both spectra. The O3 species of wadsleyite ($\delta_1 \approx 49$ ppm) appears in the ringwoodite spectrum as a small shoulder on an intense resonance at ~51 ppm, which is thus assigned to the O site in ringwoodite. At 11.7 T, this resonance appears coincidental with that attributed to the O3 species in wadsleyite, as indicated by the intensity of the corresponding peak in Figure 10b.

The overlap (partial or complete) of the ringwoodite resonance with the peaks arising from the wadsleyite impurity hinders the analysis of the spectra and the extraction of the quadrupolar and chemical shift parameters for the ringwoodite O species from the STMAS spectra. For example, although the δ_1 position of the resonance is known with reasonable precision, the δ_2 position, i.e., the center-of-mass of the second-order broadened line shape, is much more difficult to determine owing to both the overlap of the line shapes and the low signal-to-noise ratio resulting from the small amount of material available. Furthermore, any δ_2 cross-sections extracted along the ridges will contain overlapped second-order quadrupolar-broadened line shapes. However, the δ_1 position of the ringwoodite resonance is known with good accuracy at two different B_0 field strengths and these values can be used to determine P_Q and δ_{CS}, as described previously. The values extracted using this method are given in Table 1. In addition, the STMAS experiment has confirmed that the only O-containing impurity is wadsleyite. It is possible, therefore, to subtract the wadsleyite ^{17}O MAS NMR spectra in Figure 6 from those of the impure ringwoodite sample in Figure 9 to obtain spectra that only contain signals from the ringwoodite O species. These spectra, shown in Figure 11a-c at magnetic field strengths of 9.4 T, 11.7 T, and 18.8 T display reasonably well-defined second-order line shapes typical of a single O species that can be fitted to obtain values for C_Q and η. These values are given in Table 1, with the corresponding computer-generated fits shown in Figure 11d-f.

DISCUSSION

The high-resolution ^{17}O STMAS NMR spectra of the three Mg_2SiO_4 polymorphs allow the identification and assignment of eight distinct O species, three in forsterite, four in wadsleyite, and one in ringwoodite, in agreement with the number of O sites identified in the crystal structures (Hazen 1976; Horiuchi and Sawamoto 1981; Sasaki et al. 1982). The three O species in forsterite possess similar isotropic chemical shifts, but can be distinguished on the basis of their relative populations and the geometry of the immediate coordination sphere. Figure 12a shows a plot of the ^{17}O isotropic chemical shift in a variety of magnesium silicate minerals as a function of the average Si-O bond length (Ashbrook et al. 2001, 2002). The values determined for forsterite are in excellent agreement with the general trend. The four O species in wadsleyite display a wide range of isotropic chemical shifts (Ashbrook et al. 2003). The two non-bridging O species possess similar chemical shifts to those determined for forsterite. They were distinguished on the basis of their relative intensities. The bridging O species displays a much higher chemical shift that correlates with the increase in the average Si-O bond distance, as shown in Figure 12a. Finally, the five-coordinated O (coordinated only to Mg and hence not plotted) has a lower chemical shift, possibly indicative of its more ionic nature and the different coordinating nuclei. The single O species in ringwoodite (also non-bridging and coordinated to both Si and Mg) has a similar chemical shift to the non-bridging O species in forsterite and ringwoodite.

Although second-order quadrupolar broadening may pose a

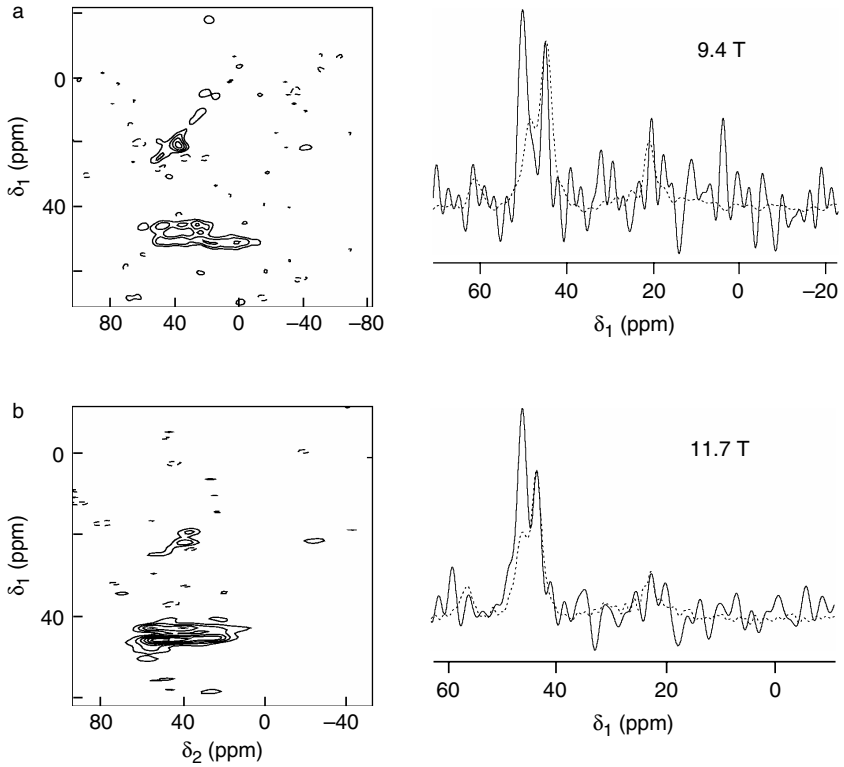

FIGURE 10. Two-dimensional ^{17}O STMAS NMR spectra of ringwoodite (plus a wadsleyite impurity), with corresponding isotropic projections (the wadsleyite isotropic projections from Figure 7 are shown dotted for comparison), recorded at (**a**) B_0 = 9.4 T and (**b**) B_0 = 11.7 T. Number of transients averaged: (**a**) 1984 and (**b**) 1920 with a relaxation interval of (**a**) 2 s and (**b**) 1 s for each of (**a**) 120 and (**b**) 100 t_1 increments of 64.6 μs. The MAS rate was 20 kHz. Total experiment times were (**a**) 132 hours and (**b**) 55 hours. Contour levels are drawn at (**a**) 30, 50, 70, and 90% and (**b**) 15, 30, 45, 60, 75, and 90% of the maximum value.

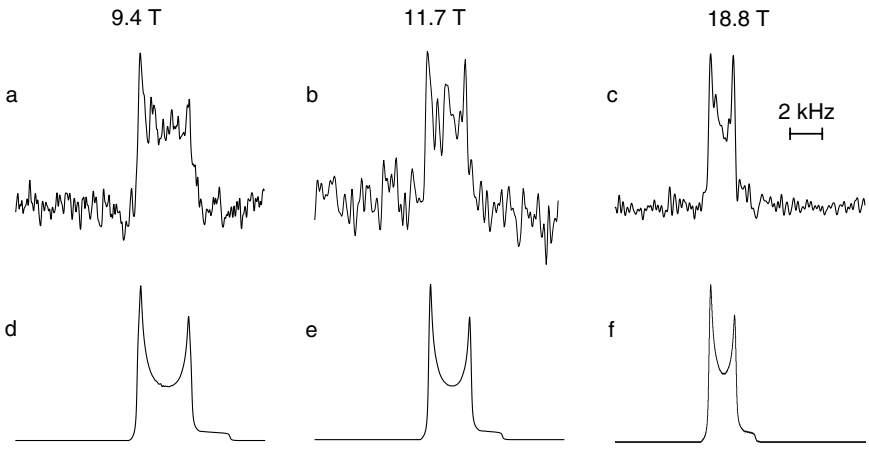

FIGURE 11. (**a**-**c**) ^{17}O MAS NMR spectra of ringwoodite at (**a**) B_0 = 9.4 T, (**b**) B_0 = 11.7, T, and (**c**) B_0 = 18.8 T obtained by subtracting the appropriate wadsleyite ^{17}O MAS NMR spectra in Figure 6 from the spectra in Figure 9. (**d**-**f**) Corresponding computer fits, yielding the C_Q and η values given in Table 1.

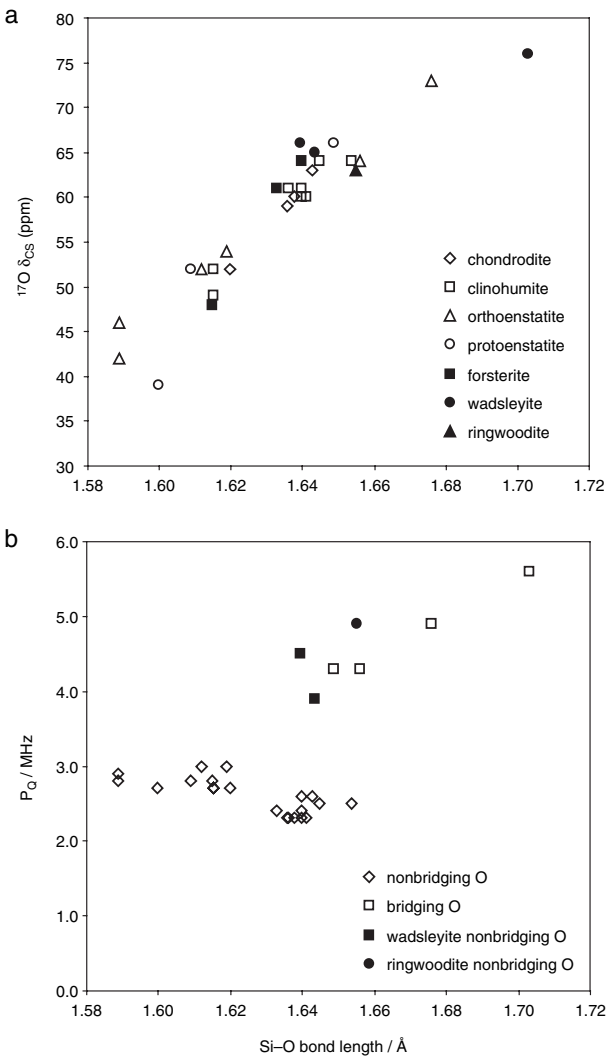

FIGURE 12. (**a**) ^{17}O isotropic chemical shift (δ_{CS}) plotted against average Si-O bond length for a variety of magnesium silicates. The values and assignments given in Table 1 have been used for forsterite, wadsleyite, and ringwoodite (highlighted with solid symbols); data for other compositions are from Ashbrook et al. (2001) and Ashbrook et al. (2002). (**b**) ^{17}O quadrupolar product (P_Q) plotted against Si-O bond length for the bridging and non-bridging O species given in (**a**). For forsterite, wadsleyite, and ringwoodite the values and assignments given in Table 1 have been used. The non-bridging O species in wadsleyite and ringwoodite have been highlighted with solid symbols to emphasize the anomalous P_Q values.

problem in the study of systems by ^{17}O NMR, the magnitude of the quadrupolar interaction can often provide a useful indication of the local structural environment. For example, many cases exist in the literature of the increased C_Q (and P_Q) encountered for bridging O species (often between 4 and 6 MHz) over those found for non-bridging O (between 2 and 3.5 MHz) (Timken et al. 1987; Kirkpatrick 1988; Xue et al. 1994; Ashbrook et al. 2002). Larger still are the quadrupolar interactions encountered in hydroxyl O species (between 6 and 8 MHz), a fact of importance for the future study of hydrous polymorphs (Kirkpatrick 1988; van Eck et al. 1999). The three O species in forsterite possess very similar P_Q values, as shown in Table 1, between 2.4 and 2.8 MHz, typical of non-bridging O species. In wadsleyite, the five-coordinate O atom has a very small quadrupolar interaction, reflecting the large degree of ionic character in its bonding. The bridging O atom in wadsleyite has the largest P_Q value (5.6 MHz), with the values of the two non-bridging O species (3.8 and 4.4 MHz) being considerably higher than those encountered in forsterite or which may be considered typical. This can be seen more clearly in Figure 12b, a plot of P_Q against Si-O bond length for the silicate minerals shown in Figure 12a. The O species fall into two distinct groups, non-bridging O with P_Q values between 2 and 3 MHz, and bridging O with P_Q values between 4 and 6 MHz. However, the two non-bridging O species in wadsleyite clearly have P_Q values that are considerably higher than those for the other magnesium silicate minerals and, in fact, are more similar to those expected for bridging O species. Similarly, the value determined for the non-bridging O atom in ringwoodite is also anomalously large, larger still than those in wadsleyite, and again is of a similar value to bridging O species, as shown in Figure 12b.

In summary, we have used ^{17}O MAS NMR to identify, characterize, and assign the distinct O species present in the three polymorphs of Mg_2SiO_4, forsterite (α-Mg_2SiO_4), wadsleyite (β-Mg_2SiO_4), and ringwoodite (γ-Mg_2SiO_4). The presence of significant second-order quadrupolar broadening hinders the extraction of this information directly from conventional MAS NMR spectra and more sophisticated methods to obtain high-resolution spectra are required. However, the synthesis of the high-pressure β and γ polymorphs produces only a few milligrams of material, and severely limits the use of many high-resolution techniques. We have demonstrated that the high sensitivity of the STMAS experiment enables high-resolution ^{17}O MAS NMR spectra to be obtained from this small amount of isotopically enriched material within a reasonable time. From these spectra, eight distinct O species (three in forsterite, four in wadsleyite, and one in ringwoodite) were identified and assigned, and their chemical shift and quadrupolar parameters determined. The only O species not coordinated to Si, the O1 species in wadsleyite, exhibits a low isotropic chemical shift and a very small quadrupolar coupling constant, reflecting its largely ionic nature. The isotropic chemical shifts of all other O species, connected to either one (non-bridging) or two (bridging) Si, display chemical shift values that agree well with a previously published correlation with Si-O bond length. However, the magnitudes of the quadrupolar interactions encountered for the non-bridging O atom in the more dense polymorphs (wadsleyite and ringwoodite) are anomalously high, with P_Q values more typical of those expected for O atoms that bridge between two Si atoms. We hope that further study of dense silicate phases coupled with an ab initio approach may offer some insight into this phenomenon. This work has provided a good basis for the study of hydrated forms of these geologically important mineral phases, through both ^{17}O and ^{1}H NMR, to further our understanding of the mechanisms of hydration.

ACKNOWLEDGMENTS

We are grateful to the Royal Society for the award of a Dorothy Hodgkin Research Fellowship (to S.E.A.), to the Australian Research Council for support, and to T.G. Sharp for supplying a sample of unenriched ringwoodite.

REFERENCES CITED

Ashbrook, S.E. and Wimperis, S. (2002) Satellite-transition MAS NMR of spin I = 3/2, 5/2, 7/2 and 9/2 nuclei: sensitivity, resolution and practical implementation. Journal of Magnetic Resonance, 156, 269–281.

——— (2004) High-resolution NMR of quadrupolar nuclei in solids: the satellite-transition magic angle spinning (STMAS) experiment. Progress in Nuclear Magnetic Resonance Spectroscopy, 45, 53–108.

Ashbrook, S.E., Berry, A.J., and Wimperis, S. (1999) Three- and five-quantum ^{17}O MAS NMR of forsterite Mg_2SiO_4. American Mineralogist, 84, 1191–1194.

——— (2001) ^{17}O multiple-quantum MAS NMR study of high-pressure hydrous magnesium silicates. Journal of the American Chemical Society, 123, 6360–6366.

——— (2002) ^{17}O multiple-quantum MAS NMR study of pyroxenes. Journal of Physical Chemistry B, 106, 773–778.

Ashbrook, S.E., Berry, A.J., Hibberson, W.O., Steuernagel, S., and Wimperis, S. (2003) High-resolution ^{17}O NMR spectroscopy of wadsleyite (β-Mg_2SiO_4). Journal of the American Chemical Society, 125, 11824–11825.

Bell, D.R. and Rossman, G.R. (1992) Water in Earth's mantle: the role of nominally anhydrous minerals. Science, 255, 1391–1397.

Bell, D.R., Rossman, G.R., Maldener, J., Endisch, D., and Rauch, F. (2003) Hydroxide in olivine: a quantitative determination of the absolute amount and calibration of the IR spectrum. Journal of Geophysical Research, 108 (B2), Art. No. 2105, doi:10.1029/2001JB000679.

Bolfan-Casanova, N., Keppler, H., and Rubie, D.C. (2000) Water partitioning between nominally anhydrous minerals in the MgO-SiO_2-H_2O system up to 24 GPa: implications for the distribution of water in the Earth's mantle. Earth and Planetary Science Letters, 182, 209–221.

Engelhardt, G. (1996) Silicon-29 NMR of solid silicates. In D.M. Grant and R.K. Harris, Eds., Encyclopedia of Nuclear Magnetic Resonance, 7, 4398–4407. Wiley, Chichester.

Frydman, L. and Harwood, J.S. (1995) Isotropic spectra of half-integer quadrupolar spins from two-dimensional magic angle spinning NMR. Journal of the American Chemical Society, 117, 5367–5368.

Gan, Z. (2000) Isotropic NMR spectra of half-integer quadrupolar nuclei using satellite transitions and magic-angle spinning. Journal of the American Chemical Society, 122, 3242–3243.

Ganapathy, S., Schramm, S., and Oldfield, E. (1982) Variable-angle sample-spinning high-resolution NMR of solids. Journal of Chemical Physics, 77, 4360–4365.

Grey, I.E., Madsen, I.C., O'Neill, H.St.C., Kesson, S.E., and Hibberson, W.O. (1999) Rietveld refinement of high-pressure $CaAl_4Si_2O_{11}$ with the R-type ferrite structure. Neues Jahrbuch für Mineralogie Monatshefte, 104–112.

Hazen, R.M. (1976) Effects of temperature and pressure on the crystal structure of forsterite. American Mineralogist, 61, 1280–1281.

Hirth, G. and Kohlstedt, D.L. (1996) Water in the oceanic upper mantle: implications for rheology, melt extraction and the evolution of the lithosphere. Earth and Planetary Science Letters, 144, 93–108.

Horiuchi, H. and Sawamoto, H. (1981) β-Mg_2SiO_4: single crystal X-ray diffraction study. American Mineralogist, 66, 658–575.

Katsura, T. and Ito, E. (1989) The system Mg_2SiO_4-Fe_2SiO_4 at high pressures and temperatures: precise determination of stabilities of olivine, modified spinel and spinel. Journal of Geophysical Research, 94, 15663–15670.

Keppler, H. and Rauch, M. (2000) Water solubility in nominally anhydrous minerals measured by FTIR and ^1H MAS NMR: the effect of sample preparation. Physics and Chemistry of Minerals, 27, 371–376.

Kirkpatrick, R.J. (1988) MAS NMR spectroscopy of minerals and glasses. In F.C. Hawthorne, Ed., Spectroscopic methods in mineralogy and geology. Reviews in Mineralogy, 18, 341–403. Mineralogical Society of America, Washington, D.C.

Kohlstedt, D.L., Keppler, H., and Rubie, D.C. (1996) Solubility of water in the α, β and γ phases of $(Mg,Fe)_2SiO_4$. Contributions to Mineralogy and Petrology, 123, 345–357.

Kohn, S.C. (1996) Solubility of H_2O in nominally anhydrous minerals using ^1H MAS NMR. American Mineralogist, 81, 1523–1526.

Kohn, S.C., Brooker, R.A., Frost, D.J., Slesinger, A.E., and Wood, B.J. (2002) Ordering of hydroxyl defects in hydrous wadsleyite (β-Mg_2SiO_4). American Mineralogist, 87, 293–301.

Kudoh, Y., Inoue, T., and Arashi, H. (1996) Structure and crystal chemistry of hydrous wadsleyite, $Mg_{1.75}SiH_{0.5}O_4$: possible hydrous magnesium silicate in the mantle transition zone. Physics and Chemistry of Minerals, 23, 461–469.

Kudoh, Y., Kuribayashi, T., Mizobata, H., and Ohtani, E. (2000) Structure and cation disorder of hydrous ringwoodite, γ-$Mg_{1.89}Si_{0.98}H_{0.30}O_4$. Physics and Chemistry of Minerals, 27, 474–479.

Llor, A. and Virlet, J. (1988) Towards high-resolution NMR of more nuclei in solids: sample spinning with time-dependent spinner axis angle. Chemical Physics Letters, 152, 248–253.

Magi, M., Lippmaa, E., Samoson, A., Englehardt, G., and Grimmer, A.R. (1984) Solid-state high-resolution Si-29 chemical-shifts in silicates. Journal of Physical Chemistry, 88, 1518–1522.

Mueller, K.T., Wu, Y., Chmelka, B.F., Stebbins, J., and Pines, A. (1991) High-resolution oxygen-17 NMR of solid silicates. Journal of the American Chemical Society, 113, 32–38.

Mueller, K.T., Baltisberger, J.H., Wooten, E.W., and Pines, A. (1992) Isotropic chemical shifts and quadrupolar parameters for oxygen-17 using dynamic angle spinning NMR. Journal of Physical Chemistry, 96, 7001–7004.

Phillips, B.L., Burnley, P.C., Worminghaus, K., and Navrotsky, A. (1997) ^{29}Si and ^1H NMR spectroscopy of high-pressure hydrous magnesium silicates. Physics and Chemistry of Minerals, 24, 179–190.

Pike, K.J., Ashbrook, S.E., and Wimperis, S. (2001) Two-dimensional satellite-transition MAS NMR of quadrupolar nuclei: shifted echoes, high-spin nuclei and resolution. Chemical Physics Letters, 345, 400–408.

Ringwood, A.E. (1975) Composition and petrology of the Earth's mantle. McGraw-Hill, New York.

Samoson, A., Lippmaa, E., and Pines, A. (1988) High-resolution solid-state NMR averaging of second-order effects by means of a double-rotor. Molecular Physics, 65, 1013–1018.

Sasaki, S., Prewitt, C.T., Sato, Y., and Ito, E. (1982) Single-crystal X-ray study of γ-Mg_2SiO_4. Journal of Geophysical Research, 87, 7829–7832.

Schramm, S. and Oldfield, E. (1984) High-resolution oxygen-17 NMR of solids. Journal of the American Chemical Society, 106, 2502–2506.

Smyth, J.R. (1994) A crystallographic model for hydrous wadsleyite (β-Mg_2SiO_4); an ocean in the Earth's interior? American Mineralogist, 79, 1021–1024.

Smyth, J.R., Kawamoto, T., Jacobsen, S.D., Swope, R.J., Herbig, R.L., and Holloway, J.R. (1997) Crystal structure of monoclinic hydrous wadsleyite [β-$(Mg,Fe)_2SiO_4$]. American Mineralogist, 82, 270–275.

Stebbins, J.F. and Kanzaki, M. (1991) Local structure and chemical shifts for six-coordinated silicon in high-pressure mantle phases. Science, 251, 294–298.

Timken, H.K.C., Schramm, S.E., Kirkpatrick, R.J., and Oldfield, E. (1987) Solid-state O-17 nuclear-magnetic-resonance spectroscopic studies of alkaline-earth metasilicates. Journal of Physical Chemistry, 91, 1054–1058.

van Eck, E.R.H., Smith, M.E., and Kohn, S.C. (1999) Observation of hydroxyl groups by O-17 solid-state multiple-quantum MAS NMR in sol-gel-produced silica. Solid-State Nuclear Magnetic Resonance, 15, 181–188.

Vega, A.J. (1996) Quadrupolar nuclei in solids. In D.M. Grant and R.K. Harris, Eds., Encyclopedia of Nuclear Magnetic Resonance, 6, 3869–3889. Wiley, Chichester.

Walter, T.H., Turner, G.L., and Oldfield, E. (1988) ^{17}O cross-polarization NMR spectroscopy of inorganic solids. Journal of Magnetic Resonance, 76, 106–120.

Winkler, B., Blaha, P., and Schwarz, K. (1996) Ab initio calculation of electric field gradient tensors of forsterite. American Mineralogist, 81, 545–549.

Xue, X., Stebbins, J.F., and Kanzaki, M. (1994) Correlations between ^{17}O NMR parameters and local structure around oxygen in high-pressure silicates: implications for the structure of silicate melts at high pressure. American Mineralogist, 79, 31–42.

MANUSCRIPT RECEIVED FEBRUARY 12, 2005
MANUSCRIPT ACCEPTED MAY 2, 2005
MANUSCRIPT HANDLED BY MICHAEL FECHTELKORD